Successful Test of a Seamless van der Waals Density Functional

John F. Dobson and Jun Wang
School of Science, Griffith University, Nathan, Queensland 4111, Australia
(Received 6 July 1998)

We report the first microscopic (RPA) calculation of the van der Waals interaction between two self-consistent jellium metal slabs—from asymptotic separations down to full contact. We also present the first test of a recently proposed seamless van der Waals density functional, which reproduces the RPA results satisfactorily at all separations. [S0031-9007(99)08626-3]

PACS numbers: 71.15.Mb, 34.20.–b, 71.45.Gm

Dispersion or van der Waals (vdW) forces play a crucial role in many situations. Examples occur in the "docking" of pharmaceutical or biological compounds, in colloidal systems, in noble-gas chemistry, and in soft matter generally. These systems typically contain so many electrons that traditional quantum methods for predicting forces are unworkable. Local and gradient density functional methods, usually employed for large systems, cannot reproduce the asymptotic vdW interaction. New algorithms for efficient calculation of vdW forces have therefore been the goal of many recent works [1–7]. While good numbers have been obtained for the case of widely separated subsystems, a practical demonstration has not yet been given of a "seamless" density-based method which works at all separations. This must include the difficult case of large systems in the overlapped and intermediate regimes, where neither traditional local-density nor existing asymptotic, perturbative van der Waals approaches are *à priori* reliable, and where vdW forces are inextricably mixed with other types of force. This Letter addresses this problem at the random-phase approximation (RPA) level, using a new, numerically exact calculation to validate a seamless van der Waals density functional proposed recently [6,7]. We treat a pair of parallel smooth self-consistent jellium slabs, and find that the correlation energies from these two methods show rather good agreement at all slab separations, from complete overlap to the asymptotic van der Waals regime.

We will first motivate the seamless functional used here. We will then describe our RPA slab calculation, which is novel in its use of smooth self-consistent density profiles at all separations. (Previous detailed nonasymptotic van der Waals calculations for the two-slab problem used artificial hard walls. See, e.g., [8,9]. They were thus inapplicable to overlapped regimes.) Finally, we will give the results from our seamless functional, and compare them with the exact numerical RPA results, and also with asymptotic semianalytic results from electron hydrodynamics.

Motivation of seamless vdW functional.—The well-known local density (LDA) [10] and generalized gradient (GGA) [11] approaches fail to produce the vdW interaction at large separations because the relevant correlations are very nonlocal functionals of the ground-state density $n(\vec{r})$. Our broad philosophy for van der Waals functionals is to use exact, or asymptotically exact, correlation energy expressions involving susceptibilities/polarizabilities. Local approximations for the susceptibility [12] or polarizability [13] then give the desired functionals. Used with Coulomb perturbation theory [14], this approach can yield good vdW energies for nonoverlapping pairs of atoms [4], but only if a drastic cutoff is imposed [1,2].

Our nonperturbative, seamless vdW functional [6,7] allows overlap and is only loosely related to that just described. It starts from the exact adiabatic connection-fluctuation dissipation (ACFD) formula

$$E_c = -\frac{\hbar}{2\pi}\int_0^1 d\lambda \int_0^\infty ds\, \mathrm{Tr}[V_{\mathrm{Coul}} * (\chi_{\lambda s} - \chi_{0s})] \tag{1}$$

for the correlation energy of an inhomogeneous system [8,15,16]. Here $\chi_{\lambda s} \equiv \chi_\lambda(\vec{r},\vec{r}',\omega = is)$ is the Kubo density-density response function of the whole system, with an additional external potential added so as to maintain the true ($\lambda = 1$) ground-state density in the presence of a modified electron-electron interaction $\lambda V_{\mathrm{Coul}} \equiv \lambda e^2/|\vec{r} - \vec{r}'|$. In (1), $[f * g](\vec{r},\vec{r}') \equiv \int f(\vec{r},\vec{r}'')g(\vec{r}'',\vec{r}')\,d\vec{r}''$ and $\mathrm{Tr}\, f \equiv \int f(\vec{r},\vec{r})\,d\vec{r}$. A direct local density approximation [12] for $\chi_{\lambda s}$ in (1) yields the LDA [7] and thus misses the vdW interaction. The interacting dynamic response $\chi_{\lambda s}$ can, however, be related to the independent-particle (Kohn-Sham) inhomogeneous dynamic response χ_{0s} by the exact Dyson-like screening equation [17]

$$\chi_{\lambda s} = \chi_{0s} + \chi_{0s} * (\lambda V_{\mathrm{Coul}} + f_{\mathrm{xc},\lambda s}) * \chi_{\lambda s}\,. \tag{2}$$

Here $f_{\mathrm{xc},\lambda s} \equiv f_{\mathrm{xc}\lambda}(\vec{r},\vec{r}',\omega = is)$ is the exchange-correlation kernel of the inhomogeneous system. While f_{xc} is not known, some information is available for the uniform electron gas [17–19]. Our seamless functional [6,7] now follows from two distinct approximations.

(a) The Kohn-Sham independent-electron response is approximated as [7]

$$\chi_{0s} \equiv \chi_0(\vec{r},\vec{r}',is) \approx \vec{\nabla}_r \cdot \vec{\nabla}_{r'} \alpha_0^{\mathrm{hom}}(n_0 = \bar{n}(\vec{r},\vec{r}'), |\vec{r} - r'|, \omega = is)\,. \tag{3}$$

Here the inputs are the actual inhomogeneous ground-state density $n(\vec{r})$ and the polarization response $\alpha_0^{\rm hom}(n_0, |\vec{r} - \vec{r}'|, \omega = is)$ of a uniform gas of density n_0. Without such an approximation one would need to calculate many one-electron wave functions to obtain χ_{0s} for the inhomogeneous system.

(b) The xc kernel is locally approximated also:

$$f_{{\rm xc}\lambda}(\vec{r}, \vec{r}', is) \approx f_{{\rm xc}\lambda}^{\rm hom}[n_0 = \bar{n}(\vec{r}, \vec{r}'), |\vec{r} - r'|, \omega = is], \tag{4}$$

and here the frequency and λ dependence could also be simplified [6,7]. The average density $\bar{n}$ used in (3) and (4) is detailed below [7].

Despite the local nature of approximations (a) and (b) above, the essential long-ranged, nonlocal aspect of the vdW interaction is retained because the nonlocality of the real-space screening integral equation (2) is retained in full. Nevertheless, our method still has a local-density character and should not be expected to give significantly better results than the LDA in compact systems where long-ranged correlations cannot occur. Gradient corrections could be added for improvement in these cases.

The present work aims to investigate the efficacy of approximation (a) for the calculation of van der Waals energies, and accordingly we simply set $f_{\rm xc} = 0$. (We will describe elsewhere the very minimal numerical changes caused by inclusion of a static local xc kernel.) Thus we work here at the RPA level, as indeed did most workers in the early days of gradient functionals. An advantage is that we can compare our functional with our numerically exact RPA solutions.

Ground state density calculation.—We carried out our tests upon twin jellium with $r_s = 2.07$ a.u.. Our model has two parallel uniform slabs of positive background, each of thickness $L = 5$ a.u., with an adjustable spacing D between their nearest edges. A neutralizing electron gas is added, resulting in a smooth ground-state electron density profile $n(z)$ and Kohn-Sham potential $V_{\rm KS}(z)$ which we solved in the self-consistent LDA [20]. We did this for a variety of separations D ranging from zero to 12 a.u. See Fig. 1, in which three cases are shown: $D = 0$ (complete contact forming a single slab of width 10 a.u., unbroken line); $D = 6$ a.u. (partial overlap, dashed line); and $D = 12$ a.u. (negligible overlap of electron clouds, dash-dotted line).

Numerically exact RPA calculation.—To find the RPA correlation energy of this system we first calculated, for each value of D, the independent-particle ("Kohn-Sham") density-density response function $\chi_{os} \equiv \chi_{\rm KS}(q_\parallel, z, z', \omega = is)$ for particles moving in the ground-state potential $V_{\rm KS}(z)$. The coordinates used are appropriate to slab geometry: $f(\vec{r}, \vec{r}', \omega) = (2\pi)^{-2} \int d^2 q_\parallel \exp \times (i[q_x(x - x') + q_y(y - y')]) f(q_\parallel, z, z', \omega)$ with $\vec{q}_\parallel = q_x \hat{x} + q_y \hat{y}$. The method of calculation involved numerical solution of 1D Schrödinger equations, and was

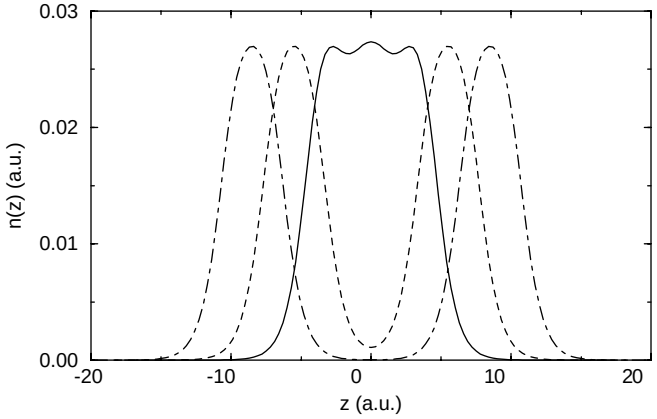

FIG. 1. Electron density for separation $D = 0$ (unbroken line), $D = 6$ a.u. (dashed line), and $D = 12$ a.u. (dash-dotted line).

essentially that described in Ref. [21]. We then solved the screening equation (2) in which the convolutions imply a separate linear 1D integral equation in z space, for each value of interaction strength λ, of frequency is, and of surface-parallel wave vector $q_\parallel$. This was treated by real-space discretization, resulting in a set of linear equations (of dimension up to 250 for the largest slab separation $D = 12$ a.u.) which we solved by LU decomposition. Equation (1) was then computed by discretizing the λ, s, and $q_\parallel$ integrations, and also the z and z' integrations implied by the convolution and trace. Typical parameters used were $dz = 0.15$ a.u., $dq_\parallel = 0.05$ a.u., $ds = 0.1$ a.u., $d\lambda = 0.3$. The D-dependent part of the resulting RPA correlation energy per unit area is shown by the open circles in Fig. 2. The RPA correlation energy of two isolated slabs has been subtracted to give $E_c^{\rm cross} \equiv [E_c(L + D + L) - 2E_c(L)]/A$. This RPA quantity measures the *cross-correlation* energy per unit area, between the slabs. For comparison, the same correlation energy quantity $E_c^{\rm cross}$ calculated in the ordinary

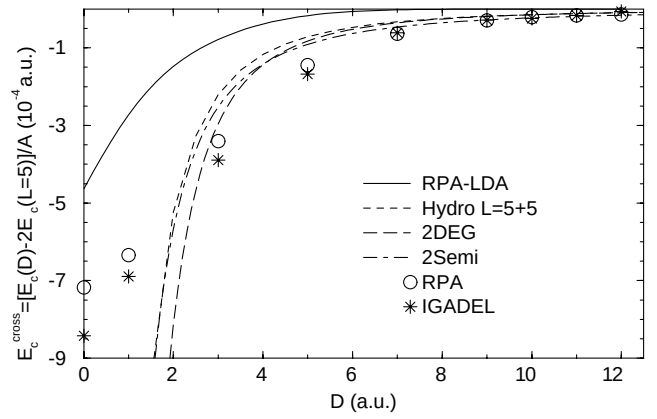

FIG. 2. Cross-correlation energy per unit area. Circles: Full RPA. Asterisks: Seamless vdW functional. Unbroken line: LDA using RPA uniform-gas e_c. Dashed lines: Hydrodynamic approximations.

LDA is shown as an unbroken line in Fig. 2 [22]. It is clear that the LDA cross correlation disappears once the ground-state densities no longer overlap, whereas in the the full RPA $E_c^{\rm cross}$ decays much more slowly.

These full RPA vdW calculations were substantial, but the screening part of the problem was made much more efficient by a rearrangement of Eq. (2) so that evaluation of $\chi_{\rm KS}$ was the time-limiting step. The cross-correlation energies plotted here are small differences of much larger total correlation energies. Nevertheless the calculations are reasonably converged, with a typical error bar, judged from variation of the above parameters, of less than half the size of the open circles as shown in Fig. 2.

Evaluation of seamless vdW functional.—Next we evaluated our approximate vdW functional for the same system. The particular form of local approximation, chosen to implement approximation (a) above in slab coordinates, was

$$\chi_{\rm KS}(z,z',q_\parallel,is) \approx \chi_{\rm KS}^{\rm IGA}(z,z',q_\parallel,is) = [\vec{\nabla}\cdot\vec{\nabla}'\alpha_{\rm KS}^{\rm hom}]_{q_\parallel,z} \equiv \left(\frac{\partial^2}{\partial z\,\partial z'} + q_\parallel^2\right)\alpha_{\rm KS}^{\rm hom}[\bar{n}^{\rm IGA}(z,z'),|z-z'|,q_\parallel,\omega=is], \tag{5}$$

where the average ground-state density is

$$\bar{n}^{\rm IGA}(z,z') = \exp\left[\frac{1}{z'-z}\int_z^{z'}\ln[n(z'')]\,dz''\right]. \tag{6}$$

In (5), the dynamic polarization response of a homogeneous gas of independent electrons is

$$\alpha_{\rm KS}(n,z,q_\parallel,is) = \frac{1}{2\pi}\int_{-\infty}^{\infty}dq_z \times \frac{1}{q_z^2+q_\parallel^2}\,\chi^{\rm Lind}(n,\sqrt{q_z^2+q_\parallel^2},is)\exp(iq_z z), \tag{7}$$

where $\chi^{\rm Lind}(n,q,\omega=is)$is the Lindhard function evaluated at imaginary frequency [23].

The choice of the particular local approximations (5)–(7) is not unique but has the following advantages: (i) The double-gradient form in (5) ensures charge conservation [4]; and (ii) the "integral geometrical Ansatz" (6) ensures [7] that no unphysical charge flow occurs across a vacuum region despite a long-ranged tail in the real-space Lindhard function. The use of (5)–(7), instead of the numerically exact calculation of $\chi_{\rm KS}$ from wave functions as in our RPA calculation, reduced the computation time by a large factor, especially for higher $q_\parallel$ values.

Comparison of seamless functional with full RPA.—Our local-density-RPA procedure [Eqs. (6), (5), (2), and (1) in that order] provides an explicit path to the correlation energy, starting with the ground-state density $n(z)$ as the only system-specific input. We thus have a genuine and highly nonlocal density functional. It is quite successful in reproducing the cross-correlation energy between two jellium slabs at all separations, as seen from the star symbols in Fig. 2 compared with the RPA (open circles). As discussed above for compact systems, the quality of the results in the fully overlapped regime is comparable to the LDA, though the error in the present case is in the opposite direction. In the separated and weakly overlapped cases, however, the present functional is dramatically better than the LDA.

Comparison with hydrodynamic theory.—To aid the understanding of our vdW results at large separation, we also used dispersionless (zero-pressure) electron-gas hydrodynamics, with self-consistent Poisson's equation. We calculated plasmon dispersion relations $\omega_j(q_\parallel)$ for coupled gases, and since the hydrodynamic response function has poles at these frequencies (with no cuts) one can show from (1) that the $T=0$ K cross-correlation energy is the change in total zero-point energy $\sum_{j,q_\parallel}\hbar\omega_j/2$ of these modes, due to proximity of the slabs. In this way one shows analytically that $E_c^{\rm cross} = -0.00501_2\hbar\times\sqrt{2\pi N_s e^2/m}\,D^{-5/2}$ for two 2D electron gases with separation D, where N_s is the areal electron number density of each gas. This is shown by the long-dashed curve in Fig. 2. Similarly by using electromagnetic boundary conditions at each jellium edge one shows for semi-infinite slabs that $E_c^{\rm cross} = -0.0110_5(\hbar\omega_P/2\sqrt{2})D^{-2}$ (dot-dashed curve) where $\omega_P/\sqrt{2}$ is the surface plasma frequency. For jellium slabs of finite thickness L, no analytic expression emerges, but our simple numerical hydrodynamic calculations gave the dashed curve in Fig. 2 (with $L=5$ a.u. to match our microscopic results). The nonhydrodynamic $E_c^{\rm cross}$ values (symbols), both from our new functional and the RPA, are clearly similar to these hydrodynamic results at large separations. In this regime of very small residual differences in a large total correlation energy, our numerics are subject to noise. In this well-separated regime one would in practice want to use asymptotic results such as the present (or more sophisticated) hydrodynamic ones. However, it is important that we have demonstrated the seamless quality of our functional: the same prescription works at all separations. It is in the weakly to moderately overlapped cases (here $1 \lesssim D \lesssim 8$) that our methods are likely to be most useful.

Note that, in contrast to some asymptotic vdW functional calculations in use for small highly confined systems such as atoms [1,2], *we have used no low-density cutoff in*

our new functional. We believe this is not needed here for two reasons. (A) At large separations D, the coupled plasmon motions which dominate $E_c^{\rm cross}$ occur in the xy directions where there is no confinement. Their dispersion can be shown to follow from Poisson's equation and a form of the f-sum rule for the independent-particle response $\chi_{\rm KS}$ of each slab, which we find is approximately satisfied [24] by our ansatz (5). (B) Also, by using the exact Lindhard response $\chi_{\rm KS}$ of the uniform gas we have included pressure effects which can be seen [4] to be absent in asymptotic vdW functionals [1,2]. These pressure effects aid in the description of motions in the z (confinement) direction which become more important at smaller separations D for the present problem.

Using a method suggested previously [6] we have now also included a local static exchange-correlation kernel $f_{\rm xc}$in the screening equation (2), and found almost no change in the cross-correlation energy plotted in Fig. 2.

Although our seamless method was worked out here for a large system, one can show analytically by the methods of Ref. [6] that it gives a cross-correlation energy of the correct vdW form $-C_6R^{-6}$ for two small systems separated by a large distance R. Preliminary tests suggest that the coefficient C_6 is overestimated by the present methods, however, so that a cutoff would be required, much as in previous nonseamless density-based approaches [2,4]. We are now testing a modified seamless method using both the ground-state density and the KS potential. The modified method also uses a self-interaction-correcting exchange-correlation kernel such that $V_{\rm Coul} + f_{{\rm xc}s,s'} = V_{\rm Coul} g_{2{\rm HF}}(\vec{r}, s; \vec{r}', s')$ where $g_{2{\rm HF}}$ is the ground-state Hartree-Fock pair distribution [25,26]. Initial indications are that these modifications make only small changes in the present slab problem, but give a greatly improved C_6 coefficient for small systems, without use of a cutoff.

In summary, we have demonstrated in Fig. 2, at the RPA level and for parallel jellium slabs, the success of our van der Waals density functional defined by Eqs. (6), (5), (2), and (1). It uses only the ground-state density as input, and is seamless in that it remains a reasonable approximation to the true RPA cross-correlation energy at all separations, from smooth overlap of electron clouds to complete separation. We also have preliminary indications that a broadly similar approach can give rather good results for small systems with a low-density cutoff, or even without a cutoff after suitable modification. Our methods do not require any excited-state quantal calculations. In this connection we should also mention time-domain vdW procedures [5] which simultaneously obtain the bare and screened response, but which still require computation of excited wave functions. Via all these means one can hope to create a truly flexible array of tools for the efficient description of dispersion forces in many-body systems.

We acknowledge discussions with N. Ashcroft, B. Dinte, W. Hanke, W. Kohn, H. Le, D. Langreth, A. Savin, B. Silvi, J. Rose, and E. K. U. Gross. We also acknowledge a grant from the Australian Research Council and support from the Queensland Parallel Supercomputing Facility.

[1] K. Rapcewicz and N. W. Ashcroft, Phys. Rev. B **44**, 4032 (1991).
[2] Y. Andersson, D. C. Langreth, and B. I. Lundqvist, Phys. Rev. Lett. **76**, 102 (1996).
[3] E. Hult, Y. Andersson, B. I. Lundqvist, and D. C. Langreth, Phys. Rev. Lett. **77**, 2029 (1996).
[4] J. F. Dobson and B. P. Dinte, Phys. Rev. Lett. **76**, 1780 (1996).
[5] W. Kohn, Y. Meir, and D. E. Makarov, Phys. Rev. Lett. **80**, 4153 (1998).
[6] J. F. Dobson, in *Topics in Condensed Matter Physics*, edited by M. P. Das (Nova, New York, 1994).
[7] J. F. Dobson, B. P. Dinte, and J. Wang, in *Electronic Density Functional Theory: Recent Progress and New Directions*, edited by J. F. Dobson, G. Vignale, and M. P. Das (Plenum, New York, 1998), p. 261.
[8] J. Harris and A. Griffin, Phys. Rev. B **11**, 3669 (1975).
[9] J. Heinrichs, Phys. Rev. B **11**, 3625 (1975).
[10] W. Kohn and L. J. Sham, Phys. Rev. **140**, A1133 (1965).
[11] J. P. Perdew *et al.*, Phys. Rev. B **46**, 6671 (1992).
[12] S. Chakravarty, M. B. Fogel, and W. Kohn, Phys. Rev. Lett. **43**, 775 (1979).
[13] K. L. C. Hunt, J. Chem. Phys. **78**, 6149 (1983).
[14] E. Zaremba and W. Kohn, Phys. Rev. B **13**, 2270 (1976).
[15] D. C. Langreth and J. P. Perdew, Solid State Commun. **17**, 1425 (1975).
[16] O. Gunnarsson and B. I. Lundqvist, Phys. Rev. B **13**, 4274 (1976).
[17] E. K. U. Gross and W. Kohn, Phys. Rev. Lett. **55**, 2850 (1985).
[18] N. Iwamoto and E. K. U. Gross, Phys. Rev. B **35**, 3003 (1987).
[19] H. M. Böhm, S. Conti, and M. P. Tosi, J. Phys. Condens. Matter **8**, 781 (1996).
[20] In our ground-state calculations we used a local Wigner xc potential, instead of the full RPA xc potential. The small resultant inaccuracies in ground-state density and potential do not greatly affect our predicted RPA energies.
[21] J. F. Dobson, Phys. Rev. B **46**, 10 163 (1992).
[22] We used the RPA correlation energy per particle of the uniform gas as input to this LDA calculation, to match our RPA calculation as closely as possible.
[23] G. D. Mahan, *Many-Particle Physics* (Plenum, New York, 1981).
[24] One can construct a simple approximation satisfying this slab geometry form of the f-sum rule exactly, but the present approximation is more readily generalized to other geometries.
[25] M. Petersilka, U. J. Gossman, and E. K. U. Gross, in *Electronic Density Functional Theory: Recent Progress and New Directions* (Plenum, New York, 1998), p. 177.
[26] M. Lein, J. F. Dobson, and E. K. U. Gross, J. Comput. Chem. **20**, 12 (1999).